Contents list available at IJRED website

International Journal of Renewable Energy Development

Journal homepage: https://ijred.undip.ac.id

Research Article

# Effect of a Detached Bi-Partition on the Drag Reduction for Flow Past a Square Cylinder

Youssef Admi *, Salaheddine Channouf, El Bachir Lahmer, Mohammed Amine Moussaoui, Mohammed Jami, Ahmed Mezrhab

*Laboratory of Mechanics & Energy, Faculty of Sciences, Mohammed 1st University, Oujda, Morocco*

**Abstract**. The objective of this research is to study the fluid flow control allowing the reduction of aerodynamic drag around a square cylinder using two parallel partitions placed downstream of the cylinder using the lattice Boltzmann method with multiple relaxation times (MRT-LBM). In contrast to several existing investigations in the literature that study either the effect of position or the effect of length of a single horizontal or vertical plate, this work presents a numerical study on the effect of Reynolds number (Re), horizontal position (g), vertical position (a), and length (Lp) of the two control partitions. Therefore, this work will be considered as an assembly of several results presented in a single work. Indeed, the Reynolds numbers are selected from 20 to 300, the gap spacing ($0 \leq g \leq 13$), the vertical positions ($0 \leq a \leq 0.8d$), and the lengths of partitions ($1d \leq Lp \leq 5d$). To identify the different changes appearing in the flow and forces, we have conducted in this study a detailed analysis of velocity contours, lift and drag coefficients, and the root-mean-square value of the lift coefficient. The obtained results revealed three different flow regimes as the gap spacing was varied. Namely, the extended body regime for $0 \leq g \leq 3.9$, the attachment flow regime for $4 \leq g \leq 5.5$, and the completely developed flow regime for $6 \leq g \leq 13$. A maximal percentage reduction in drag coefficient equal to 12.5%, is given at the critical gap spacing ($g_{cr} = 3.9$). Also, at the length of the critical partition ($Lpcr = 3d$), a Cd reduction percentage of 12.95% was found in comparison with the case without control. Moreover, the position of the optimal partition was found to be equal to 0.8d i.e. one is placed on the top edge of the square cylinder and the second one is placed on the bottom edge. The maximum value of the lift coefficient is reached for a plate length $Lp = 2d$ when the plates are placed at a distance $g = 4$. On the other hand, this coefficient has almost the same mean value for all spacings between the two plates. Similarly, the root means the square value of the lift coefficient ($Cl_{rms}$) admits zero values for low Reynolds numbers and then increases slightly until it reaches its maximum for $Re = 300$.

**Keywords:** Lattice Boltzmann Method, Square Cylinder, Control Partition, Gap Spacing, Vortex Shedding, Flow Control, Drag and Lift Coefficient



Received:24th Dec 2022; Revised: 29th May 2022; Accepted:10th June 2022 Available online: 26th June 2022

## 1. Introduction

Fluid-structure interaction is a very frequent phenomenon in our daily life. Therefore, the study of fluid flow in the presence of rough bodies represents an interesting topic of different types of investigation in various engineering applications such as flows in aircraft, submarines, automobiles, cooling of electronic components, buildings, etc. In these areas, the structures become bluff bodies characterized by loads (aerodynamic forces) caused by the strong wind-structure interaction. This can lead to malfunctioning and complex flow problems and cause structural damage to some of the systems used in these domains, which motivates the development of flow control instruments to suppress or eliminate the vortex shedding (Mooneghi *et al.*, 2016; Fatahian *et al.*, 2019; Gilliéron, 2002; Li *et al.*, 2016; Loh *et al.*, 2013).

Active control (using external energy) and passive control (without external energy) represent the two existing types of flow control devices. The passive control requires only simple instruments (flat plates, splitter plates, square rods, circular rods, etc.) to control the fluid flow and is, therefore, more economical. The partition or splitter plate is a fine rigid plate arranged parallelly to the flow. Numerous experimental and numerical studies can be found where the detached flat plate is applied as a control instrument by varying its position or length (Aabid *et al.*, 2019; Ali *et al.*, 2012; Anderson *et al.*, 1997; Apelt *et al.*, 1973, 1975; Bruneau *et al.*, 2014; Dehkordi *et al.*, 2011; Ding *et al.*, 2021; Doolan, 2009; Hassanzadeh Saraei *et al.*, 2021; S. Ul Islam *et al.*, 2015; Shams Ul Islam *et al.*, 2014; Liu *et al.*, 2016; Maruai *et al.*, 2018; Mat Ali *et al.*, 2011; Moussaoui *et al.*, 2010; Nidhul *et al.*, 2015; Ozono, 1999; Park *et al.*, 2013; Rashidi *et al.*, 2016; Roshko, 1954; Sakamoto *et al.*, 1997; Turki, 2008; Zhou *et al.*, 2005).

*Corresponding author:
Email: admiyoussef399@gmail.com (Y. Admi)

https://doi.org/10.14710/ijred.2022.43619
ISSN: 2252-4940/© 2022.The Author(s). Published by CBIORE

These studies included a large gap of Reynolds numbers, positions, and lengths of the detached flat plate showing that the vortex shedding mechanism and the physical parameters are significantly impacted. Roshko (Roshko, 1954) carried out an experimental study where a detached flat plate is inserted to eliminate the periodic vortex formation behind a circular cylinder. The author found a critical position of a detached flat plate is 2.7d.

The impact of a separated flat plate on the fluid flow past around circular cylinders is studied experimentally by Apelt *et al.* (Apelt *et al.*, 1973) for a range of Reynolds number $10^4 < Re < 5 \times 10^4$. In the case where the plate length d1 is the same as the length of cylinder d, the authors observed a noticeable reduction in drag coefficient where a minimum value has been reached. In another experimental investigation realized by Apelt and West (Apelt *et al.*, 1973), the vortex shedding was suppressed and the drag coefficient takes a constant value for d1 > 5d. A numerical study that used a flat plate to control the vortex shedding behind a square cylinder in a channel was realized by Zhou *et al.* (Zhou *et al.*, 2005) who they studied the impact of the location and the height of the plate on the fluid-structure. Turki (Turki, 2008) used the Finite Volume Method to examine the impact of a separated flat plate on the vortex shedding control behind a square cylinder for a Reynolds number ranging from 110 to 200. A slight increase in the value of the Strouhal number "St" is obtained as the gap spacing "g" increases. Likewise, they found that the St decreases with increasing g until it reaches a local minimum at about g = 2.82d for Re = 200, then, it is an increase. An investigation was carried out by Moussaoui *et al.* (Moussaoui *et al.*, 2010), which used bi-partition to control the flow past a square cylinder placed in a channel using the LBM method at Re = 150. The results obtained by the authors show that the implementation of the bi-partition was beneficial in all the cases studied. This was felt in the reduction of the drag value and fluctuating lateral forces due to vortex shedding behind the square block. Islam *et al.* (S. Ul Islam *et al.*, 2015) performed a numerical study on the impact of a downstream control plate on different flow regimes around a square rod for Re = 150 and different spacings ($0 \leq g \leq 11$). In this study, the authors classified the flow into three different regimes: the extended body flow ($0 \leq g \leq 1.53$), the reattachment flow ($1.9 < g < 4$) and the completely developed flow ($4.8 \leq g \leq 11$) flow regimes. They also indicated that the optimal gap between the square rod and the control plate is g = 0, where the drag force coefficient admits maximum reduction. Kwon and Choi (You *et al.*, 1998) performed a numerical study on the length of the detached control plate effect on the vortex shedding around circular cylinders at lower Reynolds numbers ($80 \leq Re \leq 160$). They found that the elimination of vortex shedding after a circular cylinder depended strongly on the detached flat plate and the Reynolds number and observed that the vortex shedding disappears totally when the length of the control plate exceeds the critical length. Also, experimental investigations in two-dimensional and three-dimensional flows were carried out by Anderson and Szewczyk (Anderson *et al.*, 1997) to examine the impact of a splitter plate on the nearest wake of a circular cylinder and they deduced the superposition principle. They found that the combination of some 3-D geometries and flow configuration produces a nominal two-dimensional wake. Rashidi *et al.* (Rashidi *et al.*, 2016) performed a paper review on the existing numerical and experimental studies concerning the suppression of vortex shedding and wake control methods. They classified these methods into two groups and presented the benefits, limitations, power efficiency, and specific applications of the two methods. Ali *et al.* (Ali *et al.*, 2012) varied the length of the splitter plate from 0.5 to 6 in their numerical investigation at a low Reynolds number.

Another numerical investigation was realized by Doolan (Doolan, 2009) owning on the effect of a flat plate positioned downstream of a square cylinder. The authors noted that the shear layers delivered by the edges of the square cylinder interact strongly with the flat plate. Doolan also found a significant reduction of the root-mean-square value of the lift coefficient (Clrms) compared with the case of a single square cylinder (i.e without a flat plate). Although this investigation does not include the study of the impact of the spacing between the block and the plate and the length of the flat plate. Away from the square and circular cylinders, Ozono (Ozono, 1999) carried out a numerical investigation to control the vortex shedding around the rectangular cylinder utilizing a detached flat plate. A remarkable variation of the Strouhal number was observed when varying the position of the plate.

In recent years, many researchers have used one or more rods (square or circular) to control the flow past cylinders (Alonzo-Garcia *et al.*, 2021; Bao *et al.*, 2013; Chauhan *et al.*, 2019; Chiarini *et al.*, 2021; Gupta *et al.*, 2019; Shams Ul Islam *et al.*, 2017; Vamsee *et al.*, 2014; Yu *et al.*, 2020; Zhong *et al.*, 2020; Zhu *et al.*, 2020). A reduction in the range of 10% to 15% in drag coefficient has been reported by Gupta (Gupta *et al.*, 2019) by using a small control rod for Re = 100. Bao and Tao (Bao *et al.*, 2013) used two control plates disposed parallel to decrease the fluid force on a circular rod. The authors noted that the retarding of vortex shedding on the principal rod is more important compared to the case of a single control plate. They concluded that the position and length of the plate have a significant role in the flow control behind the principal rod. These findings are confirmed by the numerical simulations performed by Vamsee *et al.* (Vamsee *et al.*, 2014) related to the influence of one or two control plates situated upstream and/or downstream of a single square rod. Islam *et al.* (Shams Ul Islam *et al.*, 2017) used a 2D lattice Boltzmann method to simulate flow past on the principal cylinder with separate control positioned at various positions for Re equal 160, whereas the spacing ratio between these cylinders was taken in the range from 0.5 to 8. A reduction of 8.3% was obtained by the authors for the mean value of the drag coefficient (Cdmean). This result was obtained when both control rods were located at an upstream position. Whereas, when these rods were situated at a downstream location, the reduction became 51%. For four control rods situated upstream and downstream of a square rod, a reduction of 50.8% was obtained.

In the literature, many investigations have been performed on the flow through a square cylinder with one passive control device at various gap spacing and different lengths of control devices. Thus, the main objective of this investigation is to present a detailed study on the reduction of vortex shedding and the reduction of the fluctuation amplitude of the drag and lift of a square cylinder by adding two passive control devices.

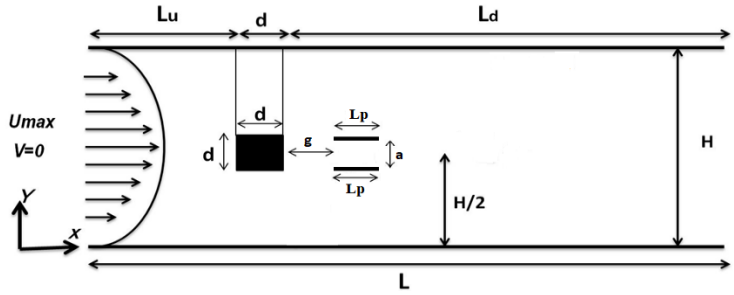


**Fig. 1.** The configuration of the physical problem

## 2. Presentation of the physical problem and boundary conditions

The physical problem under consideration is drawn in Figure1. It consists of a 2D channel of length-height dimension "L = 37d"-"H = 11d", including a square cylinder followed by two control partitions. The square cylinder of size "d" is situated at Lu = 6.0d from the entry and Ld = 30.0 d from the outlet. The two controlling partitions of length "Lp" and thickness "h=0.02d" are placed horizontally behind the cylinder with gap space noted "g". The vertical distance between the two partitions is "a".

Consider that the fluid enters with a parabolic velocity in the horizontal direction($u = U_{max}[1 - ({}^{y}/_{H})^2$) while the vertical component is assumed to be zero (v= 0).

The implementation of boundary conditions is very essential for the stability and precision of the LBM numerical approach. Indeed, the Bounce-Back boundary conditions (Bouzidi *et al.*, 2001; Moussaoui *et al.*, 2010) are applied to define the inconnu distribution functions at solid boundaries, from the known functions, by the following relation:

$$f_i(\vec{x}_B, t) = f_{\bar{i}}(\vec{x}_B, t) \quad (1)$$

Where $f_i(\vec{x}_B, t)$ is the inconnu distribution function at the wall node ($\vec{x}_B$) and $f_{\bar{i}}(\vec{x}_B, t)$ is the knowing function in the contrary direction to $f_i(\vec{x}_B, t)$.

At the inlet of the channel, the boundary conditions of Zou and He are applied (Zou *et al.*, 1997) since the flow is completely developed with a parabolic velocity profile.

## 3. Description of the numerical method

The numerical approach employed for the simulation of the wake structures and aerodynamic forces exerted on the square block in the presence of the dual detached partition is the lattice Boltzmann method with multi-relaxation time (MRT-LBM) with the uniform grids (740×220). The choice of this method is based on its flexibility, ease of implementation, parallel computational advantages, and its diverse applications. Indeed, many researchers (Admi *et al.*, 2022; Admi *et al.*, 2020, 2022c, 2022a, 2022b; Benhamou *et al.*, 2020; Benhamou, *et al.*, 2022; Benhamou & Jami, 2022; Bhatnagar *et al.*, 1954; D'Humières *et al.*, 2002; Lahmer, Admi, *et al.*, 2022; Lahmer, Benhamou, *et al.*, 2022; Lallemand *et al.*, 2000; Mezrhab *et al.*, 2010; Mohamad, 2011; Moussaoui *et al.*, 2010, 2011, 2019, 2021; Qian *et al.*, 1992; Admi *et al,* 2022) performed to simulate diverse physical phenomena such as fluid flow, wave propagation, heat exchange, etc by using the LBM method. For precision and convergence reasons, the D2Q9 model (Figure 2) is utilized in this paper (Mohamad, 2011).

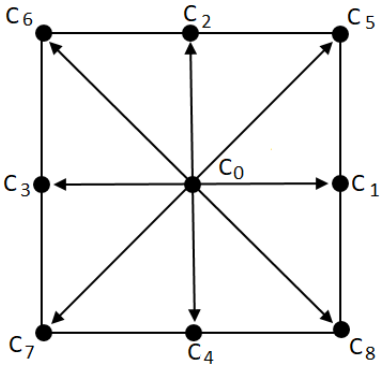


**Fig. 2**. Structure of the D2Q9 model

The spatial-temporal evolution of the LBE is defined by the development of the function fi representing the density distribution of particles:

$$f_i(x + c_i\Delta t, t + \Delta t) = f_i(x, t) + \Omega(f), i = 0,1,\ldots,8 \quad (2)$$

Where Ω represents the operator of the collision developed by D'Humières based on the LBM-BGK model. The development proposed by D'Humières (D'Humières *et al.*, 2002) permits to write the previous equation as follows:

$$f_i(x + c_i\Delta t, t + \Delta t) - f_i(x, t) = M^{-1} \times S_i \times \left(m_i(x, t) - m_i^{eq}(x, t)\right), i = 0,1,\ldots,8 \quad (3)$$

Where $S$, $m$ and $m^{eq}$ represente respectively the relaxation matrix, the moment and the equilibrium moment vectors. The $M^{-1}$ denotes the inverse matrix of the transformation matrix $M$. $M^{-1}$ and $M$ are $(9 * 9)$ matrices. They permit to link the vector $f = (f_0, f_1, f_2, \ldots, f_n)^T$ to the vector $m = (m_0, m_1, m_2, \ldots, m_n)^T$ via the linear transformations:

$$m = Mf \text{ and } f = M^{-1}m \quad (4)$$

The matrix $M$ of order 9 is explicitly given by (Mohamad, 2011).

After the collision, two moments are locally conserved: the density ($m_0$) and the quantity of movement ($m_3$, $m_5$). The other moments ($m_1$, $m_2$, $m_4$, $m_6$, $m_7$, $m_8$), named respectively, the kinetic energy, the energy square, the components of the energy flux, and the components of the viscous stress tensor, relax linearly towards their equilibrium values. These non-conserved moments are defined by:

$$m^c = m + S.(m^{eq} - m) \quad (5)$$

Where $m^c$ is the moments after the collision and $m^{eq}$ is the equilibrium moments such as:

$$m^{eq} = (\rho, e^{eq}, \varepsilon^{eq}, j_x, q_x^{eq}, j_y, q_y^{eq}, p_{xx}^{eq}, p_{xy}^{eq})^T \quad (6)$$

The equilibrium moments $m^{eq}$ are defined by (Mohamad, 2011).
In compact notation, the $S$ matrix can be expressed as:

$$S = \mathrm{diag}(s_0, s_1, s_2, s_3, s_4, s_5, s_6, s_7, s_8) \quad (7)$$

The relaxation times used are those mentioned in the reference (Frisch *et al.*, 1986).We have chosen $s_0 = s_3 = s_5 = 1$, $s_1 = s_2 = 1.4$, $s_4 = s_6 = 1.2$ and $s_7 = s_8 = 1/(3\nu + 0.5)$, where ν is the kinematic viscosity of the simulated fluid.
The density ρ and the momentum ρu are calculated by:

$$\rho = \sum_{i=0}^{8} f_i \ , \quad \rho u = \sum_{i=0}^{8} c_i f_i \quad (8)$$

## 4. Validation

To assure the reliability and the exactitude of our LBM-MRT code, several validation results with existing numerical and experimental results in the literature are presented in this paper. Firstly, a numerical simulation of the fluid flow around a square cylinder without control and with a blocking ratio H/d = 8 has been performed. The results obtained in this validation work are compared with those found by Breuer *et al.* (Breuer *et al.*, 2000), for which they applied two different methods, namely the finite volume method (FVM) with *560×340* non-uniform grid and the Lattice Boltzmann automata (LBA) using *2000×320* uniform grid.

Figure 3 displays the U and V velocity curves along the x and y axes respectively, for Reynolds number *Re = 100*. The results are very close to those of Breuer *et al.* with a difference of less than 1.69%.

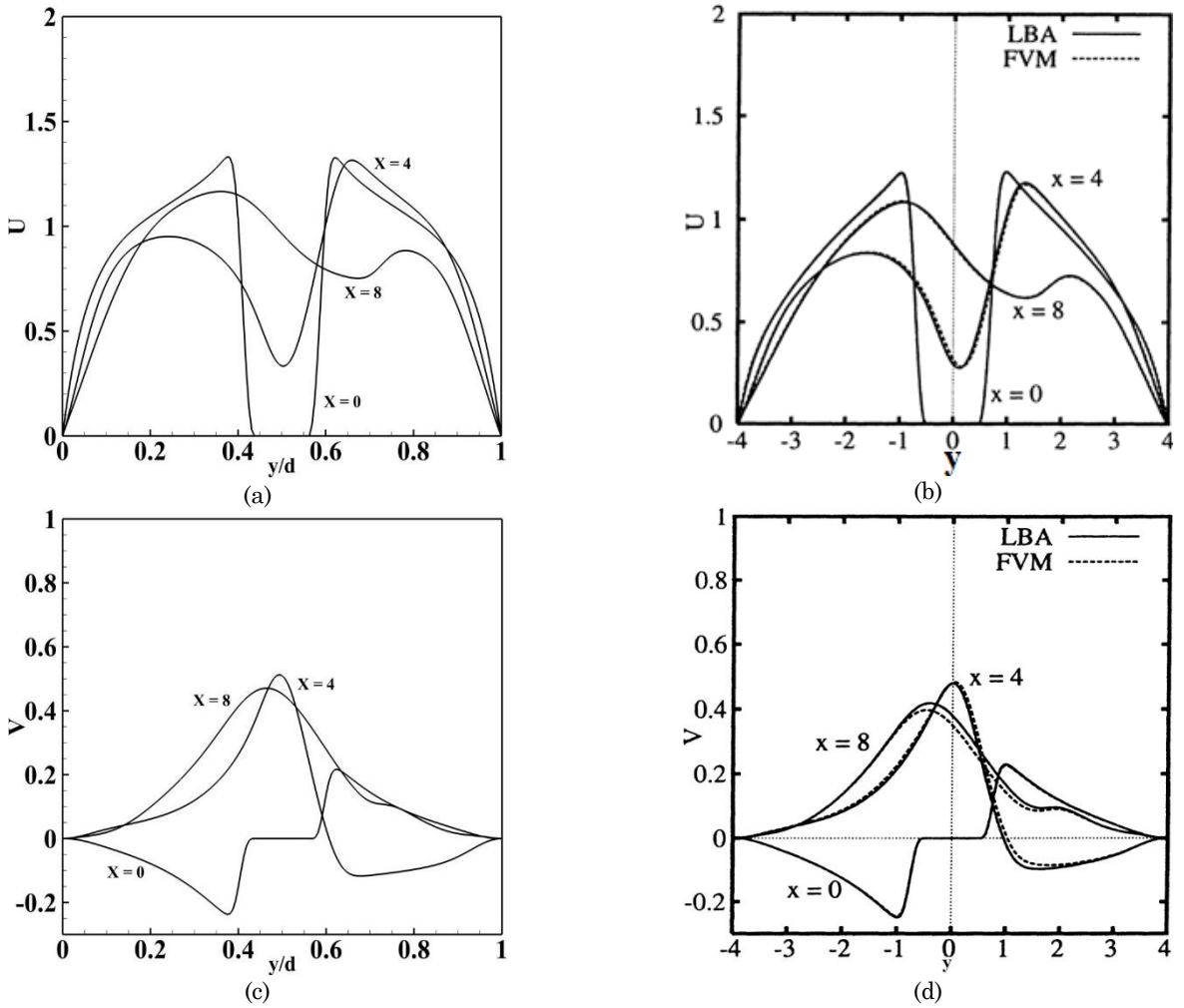


**Fig. 3**. Velocity profiles comparison for Re =100, (a and c) Our results, (b and d) Reference (Breuer *et al.*, 2000)

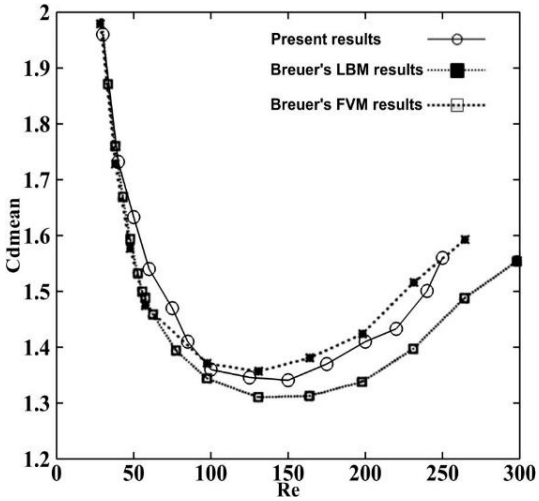


**Fig. 4**. Average drag coefficient comparison for a single obstacle.

Figure 4 shows the time-averaged drag coefficient $Cd_{mean}$ as a function of the Reynolds number ($20 \leq Re \leq 300$). The drag coefficient Cd is one of the most important parameters for the flow around an obstacle. This coefficient is defined by the following equation:

$$Cd = \frac{2 \times F_D}{\rho . U_{max}^2 . D} \quad (9)$$

From this figure, it can be seen that the $Cd_{mean}$ values compare favorably with those of Breuer *et al.* (Breuer *et al.*, 2000)

The exactness of our numerical code is also verified in the case of flow around a square cylinder controlled by a flat plate located downstream. Figure 5 illustrates the variation of the average drag coefficient for various gap spacings ($0 \leq g \leq 11$) at a fixed Reynolds number *Re = 150*. This figure shows that there is very good agreement between our results and those found experimentally by Okajima *et al.* (Okajima A, 1982) and those obtained numerically by Islam *et al.* (S. Ul Islam *et al.*, 2015). Note that we found the almost same values as Turki *et al.* (Turki, 2008) for the same grid (500×80).

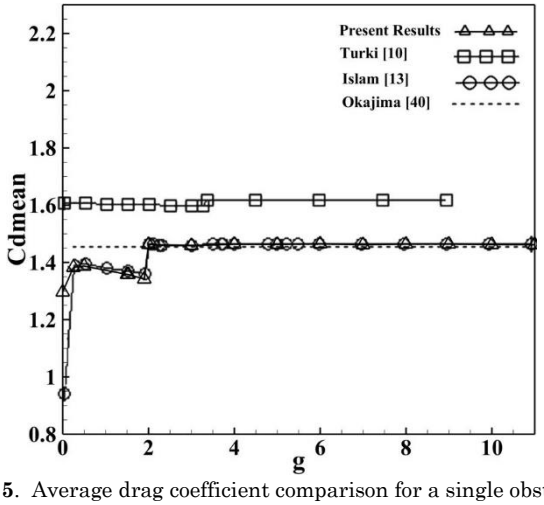


**Fig. 5**. Average drag coefficient comparison for a single obstacle with control partition.

## 5. Results and discussion

Firstly, the distance between partitions, length, and position of partitions are fixed at $a = 0.8d$ and $Lp = g = 1d$. The effects of *Re* on flow patterns, drag coefficient, and $Cl_{rms}$ are studied. Secondly, the effect of gap spacing between the square cylinder and the two partitions is studied for a fixed length of partitions ($Lp = 1d$), the distance separating the two control partitions ($a = 0.8d$), and Reynolds number ($Re = 150$). Thirdly, the length of the partitions is varied for the gap spacing ($g = 4$) and the Reynolds number ($Re = 150$). Finally, the effect of the distance separating the two control partitions is treated for the lengths ($Lp = 1d$), the spacing gap ($g = 1$), and the Renolds number (Re = 150).

### *5.1 Effect of Reynolds number*

#### *5.1.1 Regime flow*

In this part, the effect of the Reynolds number on the velocity contours is performed. For this purpose, the length of the two control partitions is fixed at Lp = 1d. The partitions are positioned behind the top and bottom edges of the cylinder at a distance of g = 1. As mentioned earlier, several studies exist in the literature that treat the flow of fluids around a square cylinder with and/or without control partition (Youssef Admi *et al.*, 2022b; Ali *et al.*, 2012; Breuer *et al.*, 2000; Doolan, 2009; Hassanzadeh Saraei *et al.*, 2021; S. Ul Islam *et al.*, 2015; Shams Ul Islam *et al.*, 2014; Mat Ali *et al.*, 2011; Moussaoui *et al.*, 2010; Nidhul *et al.*, 2015; Saha *et al.*, 2003; Sohankar *et al.*, 1998; Turki, 2008; Zhou *et al.*, 2005). Among these studies, we find those that address the effect of the Reynolds number on several physical parameters (Nidhul *et al.*, 2015; Sohankar *et al.*, 1998). Sohankar *et al.* (Sohankar *et al.*, 1998) have found that at $Re \leqslant 150$ the wake of a square cylinder is laminar, two-dimensional and characterized by the primary spanwise Kármán vortices. They have also concluded that the wake shows spanwise secondary instability and becomes three-dimensional in the range between Re = 150 and 200. Saha *et al.* present a numerical study of the spatial evolution of vortices and the transition to three-dimensionality in the wake of a square cylinder. The study is considered for a range of Reynolds numbers $150 \leq Re \leq 500$. The authors find that the transition to three-dimensionality occurs at Reynolds numbers between 150 and 175. Likewise, they find that secondary vortices of the A-mode persist over the Reynolds number range of 175 to 240. On the other hand, at a Reynolds number of about 250, the secondary vortices of mode B are present. Also, Nidhul *et al.* (Nidhul *et al.*, 2015)numerically investigated the flow past a square block with and without a detached flat plate by using CFD fluent. Their results show that for Re > 40, the flow past on the square cylinder becomes unstable and results in an oscillating flow whose oscillation amplitude increases downstream. This exerts a force on the cylinder in a lateral direction. These forces are reduced using the separated plate that suppresses the vortex shedding. Zhou *et al.* (Zhou *et al.*, 2005) performed a numerical study on the reduction of fluid forces acting on a square cylinder in a two-dimensional channel using a control plate. It is well known that the vortex shedding phenomenon can be significantly modified for uniform flows passing a bluff body at different Reynolds numbers. The vortex structure behind the cylinder in a shear flow can also depend on the Reynolds number.

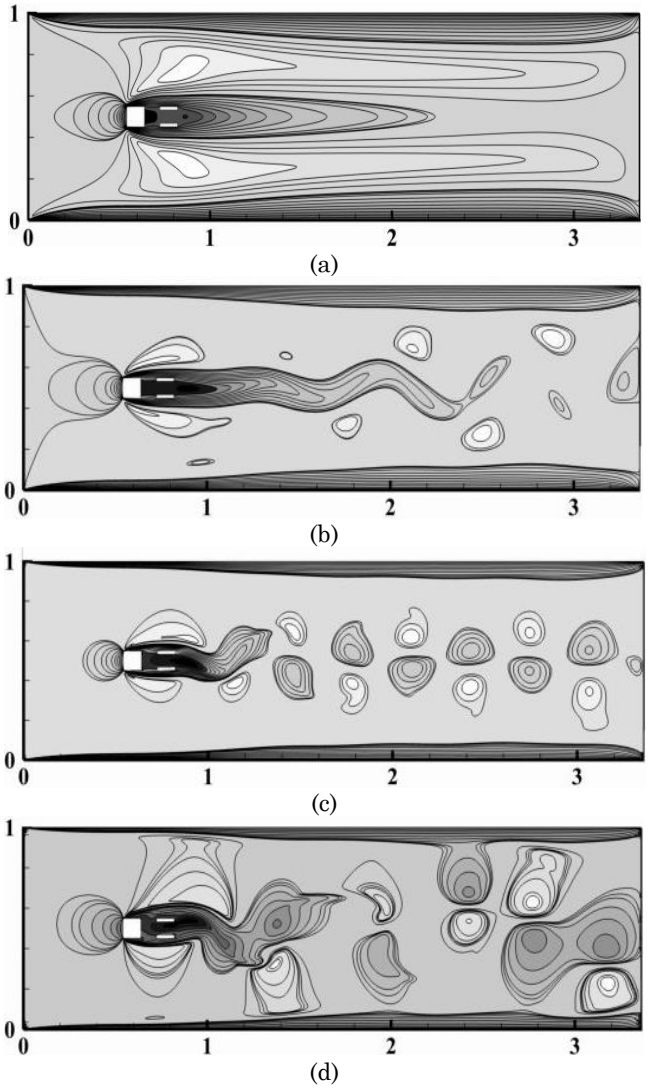


**Fig. 6.** Visualization of instantaneous flow velocity contours for different Reynolds number: (a) Re = 20; (b) Re = 65; (c) Re = 150; (d) Re = 300.

In this part, the effect of the Reynolds number on the velocity contours is performed. For this purpose, the length of the two control partitions is fixed at Lp = 1d. The partitions are positioned behind the top and bottom edge of the cylinder at a distance of g = 1. Figure 6 displays the velocity contours for various Reynolds values (Re = 20, 65, 150, 300) characterizing different flow regimes. The results obtained show that the flow is stable and perfectly symmetrical about the horizontal axis of the channel for low values of Reynolds number (Re < 60).

A detachment of a few small vortices appeared just downstream of the cylinder at a critical Reynolds number *Re* = 65. In this case, the previously obtained stability disappears and the flow is characterized by low amplitude undulations (Figure 6-b). When *Re* is in the interval (100 < Re < 250), a strong generation of vortices is observed along the channel and the regime becomes periodically variable in time. i.e., there is an alternation of positive and negative vortices generated by the lower and upper edges of the square cylinder. For high Reynolds numbers (Re > 270), the periodicity and symmetry, obtained before, disappear and the regime becomes intense. This instability is due to the great interaction between the shear layers produced by the ends of the cylinder and the control partitions. This causes oscillations of the flow behind the cylinder and behind the partitions. This gives rise to the formation of vortices of different sizes that propagate randomly in the flow direction.

### *5.1.2 Force statistics*

The effect of the Reynolds number on the average drag coefficient (as well as on the temporal drag coefficient) and the mean square value of the lift coefficient are studied in this section. Some previous works that have studied the effect of the Reynolds number on the average drag coefficient around a square cylinder without and with a single control partition are cited here(Breuer *et al.*, 2000; Feng *et al.*, 2001; Shams Ul Islam *et al.*, 2014). Breuer *et al.*, 2000) used two methods (LBM and FVM) to study the confined flow around a square cylinder mounted inside a horizontal channel with a blocking ratio ß =1/8 and for a range of Reynolds numbers between 0.5 and 300. For Re < 60, the authors find an excellent agreement between LBA and FVM results for the length of the recirculation region, while small deviations are detected for the drag coefficients in this range. Likewise, they calculated the drag coefficient for the other Reynolds number ranges and found that the drag coefficient of a confined cylinder also shows a local minimum at Re 150.

Islam *et al.* (Shams Ul Islam *et al.*, 2014) performed a numerical study of the flow along a square cylinder in a two-dimensional channel with a detached flat plate. They use a detached flat plate downstream to control the flow around and behind the square cylinder. The study of vortex generation, time trace analysis of drag and lift coefficients, and root mean square (rms) value of drag and lift coefficients are performed using the Boltzmann lattice method for a range of Reynolds numbers from 75 to 200. They found a reduction of more than 90% in the rms value of drag and lift coefficients for a reduced spacing, regardless of the Reynolds number. While wake development and vortex formation behind the square cylinder depend significantly on the Reynolds number.

Figure 7-a displays the variation of the mean drag coefficient as a function of the Reynolds number. From this figure, it can be seen that the value of $Cd_{mean}$ is higher for low Reynolds numbers and it decreases with the increase of this number until it reaches a minimum at *Re* = 250. Then, it increases slightly until it obtains an almost stable value between *Re* = 270 and 300. It is well known that the drag force is the resultant of the viscous force due to the friction of a moving object flowing in the opposite direction of the fluid (i.e., it represents the resistance of an object in a fluid). Therefore, as viscosity increases, the $Cd_{mean}$ coefficient also increases. Thus, a viscous fluid means that the Reynolds number is low and therefore higher Cd values are obtained. More Re increases, more $Cd_{mean}$ decreases. This decrease reaches its minimum at Re = 250, where the flow is detached from the body by the two control partitions. After that, a strong vortex generation around the obstacle is observed, which causes a disturbance of the flow and increases the mean value of the drag coefficient.

The calculation of the average lift coefficient is not of interest since the latter admits a zero value for all the Reynolds numbers processed. It is, therefore, preferable to calculate its root mean square value $Cl_{rms}$. Figure 7-b illustrates the variation of this coefficient as a function of *Re*. We observe that $Cl_{rms}$ gradually increase with the increase of Reynolds number.

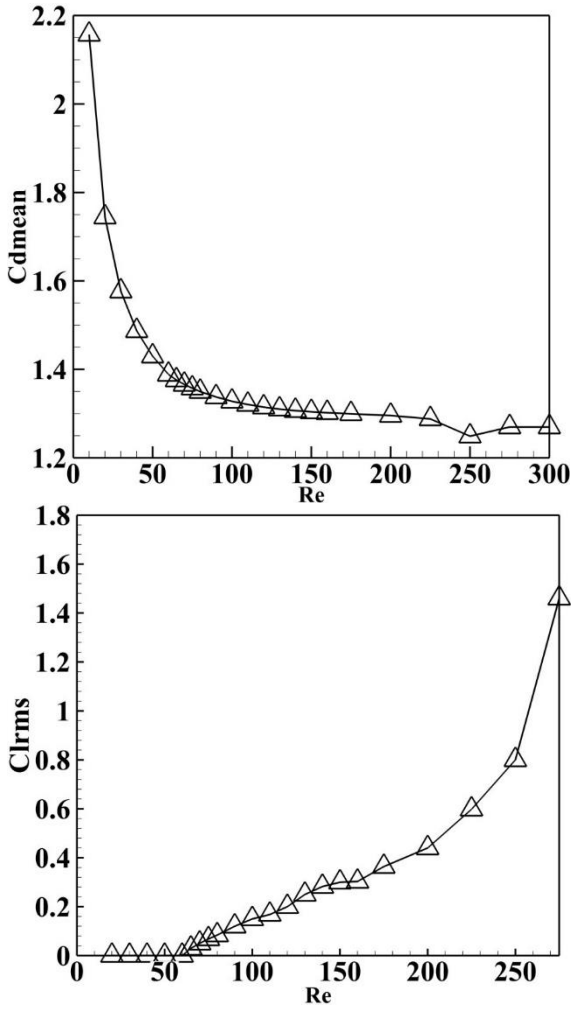


**Fig. 7.** The evolution of the drag coefficient and root-mean-square of the lift coefficient as a function of Reynolds number.

### *5.2 Effect of the gap spacing*

#### *5.2.1 Regime flow*

The effect of the distance between the principal cylinder and the control partition (gap spacing) is widely studied in the literature (S. Ul Islam *et al.*, 2015; Mat Ali *et al.*, 2011; Rashidi *et al.*, 2016). Islam *et al.* (S. Ul Islam *et al.*, 2015) performed a numerical study on the impact of a downstream control plate on different flow regimes around a square rod for Re = 150 and different spacings ($0 \leq g \leq 11$). In this study, the authors classified the flow into three different regimes: the extended body flow ($0 \leq g \leq 1.53$), the reattachment flow ($1.9 < g < 4$) and the completely developed flow ($4.8 \leq g \leq 11$) flow regimes. Ali *et al.* (Mat Ali *et al.*, 2011) used a detached flat plate downstream of the square cylinder to study a wake alternation for Re = 150. They observed two distinct types of flow regimes within the gap spacing between the cylinder and splitter plate and after this plate. An investigation review was conducted by Rashidi *et al.* (Rashidi *et al.*, 2016) In this study, the authors discuss existing studies on different methods of controlling the destructive behaviour of the wake and suppression of vortex ejection behind bluff bodies. Likewise, this study presents a discussion on the advantages, limitations, energy efficiency, and specific applications of two existing control methods. Figure 8 illustrates the velocity contours in the wake of the cylinder in the presence of double detached plates at various gap spacings. For a narrow spacing ($0.25 \leq g \leq 3.9$), the extended body regime is clearly observed. The separate free shear layers of the extremity of the square block are attached to the two control plates. Consequently, the alternating vortex shedding is only observed after the plates (as for a single bluff body case). In this case, the positive and negative vortices produced by the upper and lower edges of the cylinder are quickly reattached to the control plates. Therefore, an alternating generation of vortices behind the two detached flat plates is clearly observed without any fusion or distortion. It is noted that for $g < 3.9$, all simulation cases have almost similar characteristics. Another flow regime is presented in figures 10 a-d where the spacing g varies from 4 to 5.5. This is the attachment flow where the distance between the block and the plates exceeds a crucial gap value ($g = 3.9$). The shear stress layers detached by the square cylinder are developed and then rapidly reattached to the control partitions. Consequently, the vortex shedding is only observed behind the detached partitions.

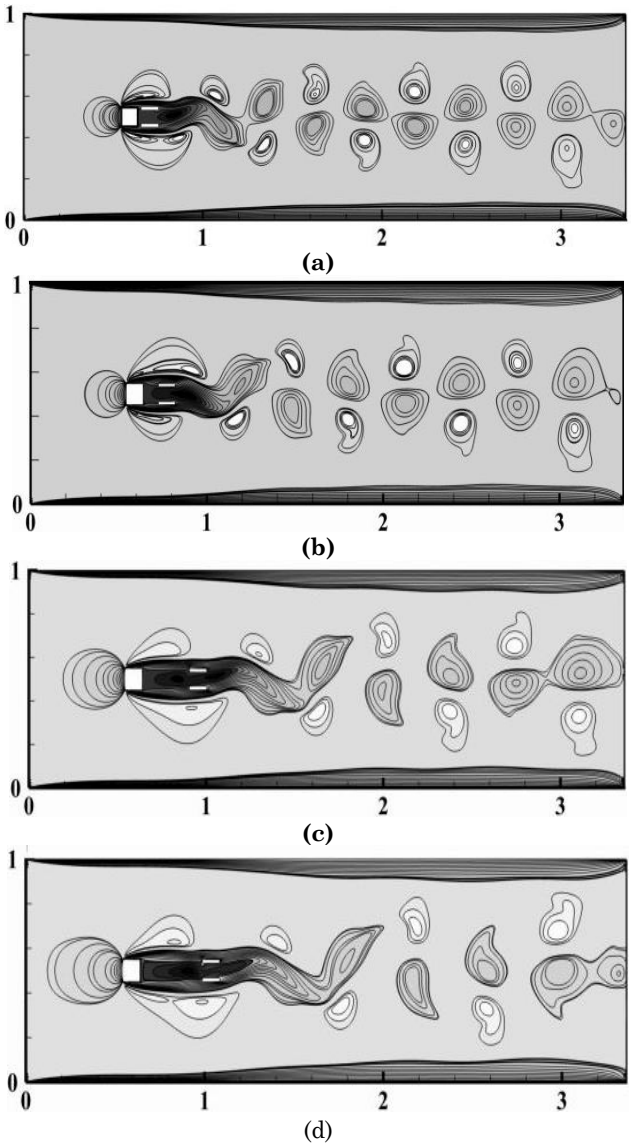


**Fig. 8.** Visualisation of instantaneous flow velocity contours for $0.25 \leq g \leq 3.9$: (a) g = 0.25; (b) g = 1; (c) g = 3; (d) g = 3.9.

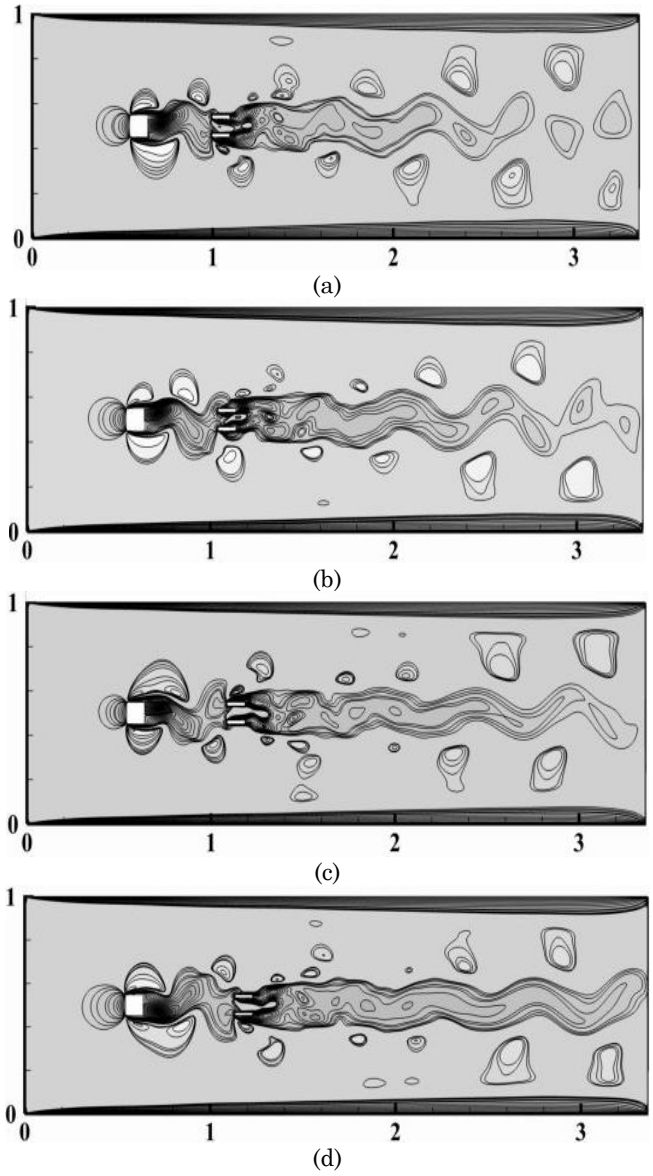


**Fig. 9.** Visualisation of instantaneous flow velocity contours for 4≤ g <6: (a) g = 4; (b) g = 4,5; (c) g = 5; (d) g = 5.5

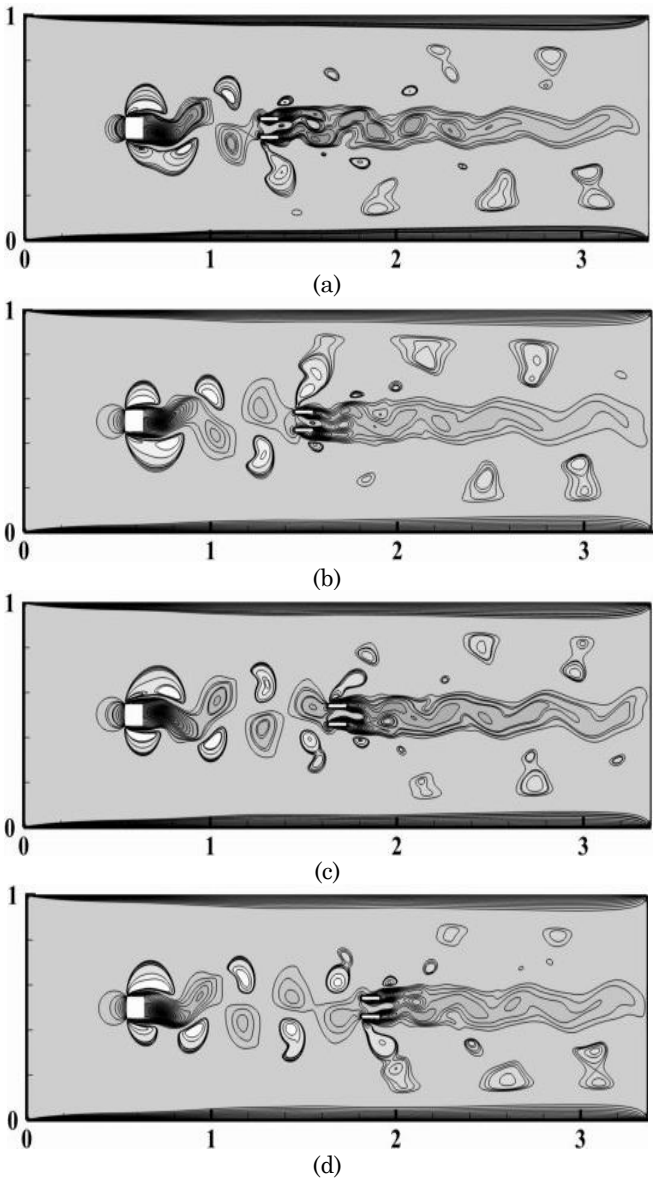


**Fig. 10.** Visualisation of instantaneous flow velocity contours for 7≤ g ≤13: (a) g = 7 (b) g = 9; (c) g = 11; (d) g = 13

For this range of g, a strong interaction of the shear layers with the control partitions is observed. Thus, it affects the length and size of the wake. Figure 9 a-d shows that the number and size of vortices shedding behind the control plates change completely compared to the previous case. Generally, in this flow regime, the form of the wake is enlarged just behind the plates, which reinforces the vortices shedding of the square cylinder. Consequently, the mean value of the drag coefficient is slightly elevated than the corresponding value for a unique cylinder (i.e. without control partitions).

Figure 10 illustrates the third flow regime, named a completely developed flow regime. In this case, the vortex evacuated in the intermediary distance is totally developed. Also, one can clearly observe an alternation of positive and negative vortices produced from the top and bottom edge of the block almost as the case was using the square cylinder without control. However, the wake behind the detached partitions is characterized by the undulating behaviour and the formation of the vortex of different sizes.

### *5.2.2 Force statistics*

Likewise, the fluidic forces exerted on the square cylinder are influenced by the variation of the gap spacing. Indeed, Islam *et al.* (S. Ul Islam *et al.*, 2015) also indicate that the optimal gap between the square cylinder and the control plate is g = 0 (the plate is attached to the square cylinder) where the drag force coefficient admits a maximum reduction. Zhou *et al.* (Zhou *et al.*, 2005) present a numerical study on the reduction of fluid forces acting on a square cylinder (prism) in a two-dimensional channel using a control plate. They find that not only is the drag on the square cylinder significantly reduced by the control plate, but also the fluctuation of the lift is suppressed. The optimal position of the control plate to minimise the drag on the square cylinder is found for each control plate height. They also find that there is an optimal position and size for the upstream plate to effectively suppress lift. Likewise, Doolan (Doolan, 2009) presents a numerical study of the flow around a single square cylinder (prism) controlled by an infinitely thin plate at Re = 150. Doolan (Doolan, 2009) finds that the addition of an infinitely thin plate in the near-wake has resulted in fundamental

changes in the flow field. Indeed, the main characteristics of the flow between the cylinder and the plate are strong secondary vortices at the leading and trailing edges of the plate and an inverted flow environment above the plate. Also, Doolan (Doolan, 2009) finds that the force applied on the square cylinder was significantly reduced. However, the magnitude of the lift coefficient on the downstream plate was found to be the same as for the simple square cylinder.

Figures 11, 12, and 13 illustrate the time plot of the drag coefficient (Cd) for various gap spacing ranges. For $0.25 \leq g \leq 3.9$, the temporal variation of Cd of the square cylinder has an irregular profile, resulting from the short distance between the square and the plates. The shear layers produced by the block are partially or totally attached to the detached partitions. Note that for the cases where $g < g_{cr}$ show almost identical characteristics. Also, a reduction in the amplitude of the drag coefficient is observed with increasing spacing. From the graphs in Figure 11, it can be observed that the average value of the drag coefficient decreases from 1.296 for g = 0.25 to 1.256 for g = 3.9. This is justified by the variation in the length and width of the detached vortices behind the control plates. While there is a remarkable increase in the value of the drag for g between 4 and 5.5. This is clearly explained by the behavior of the velocity wake structure behind the plates. In this case, the shear layers crash with the control plates, which disturbs the intermediate zone between the square cylinder and the partitions. This increases the forces applied to the back surface of the block. Similarly, this range represents a transition from an irregular regime ($g \leq 3.9$) to a regular regime ($g \leq 5.5$). For elevated values of g ($6 < g < 13$), regular variations in the drag coefficient are observed; this is due to the large spacing existing between the square cylinder and the detached control plates allowing a regular development of the shear layers delivered by the upper and lower face of the square cylinder.

The comparison of graphs showing the temporal variation of the drag coefficient in this case with those obtained previously (tie flow) shows that they have the same profile but the amplitude of the fluctuation for all spacings in the tie flow regime is greater than in the fully developed flow regime. The amplitude of the drag coefficient is slightly higher at g = 5. Then it decreases until g = 6; thereafter, an almost constant behaviour is observed from g = 7 to g =13. It should be noted that some cases are not presented in this article.

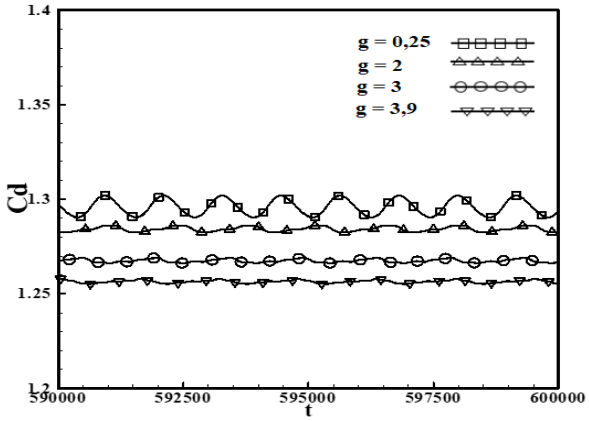


**Fig. 11.** Time-trace of the drag coefficient in the case of an extended body regime

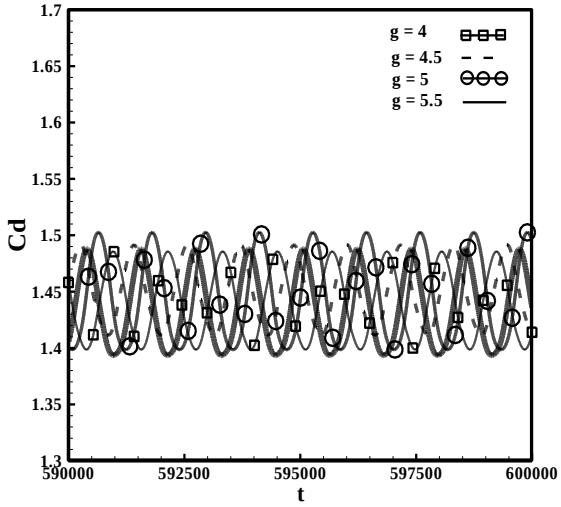


**Fig. 12.** Time-trace of the drag coefficient in the case of reattachment flow regime

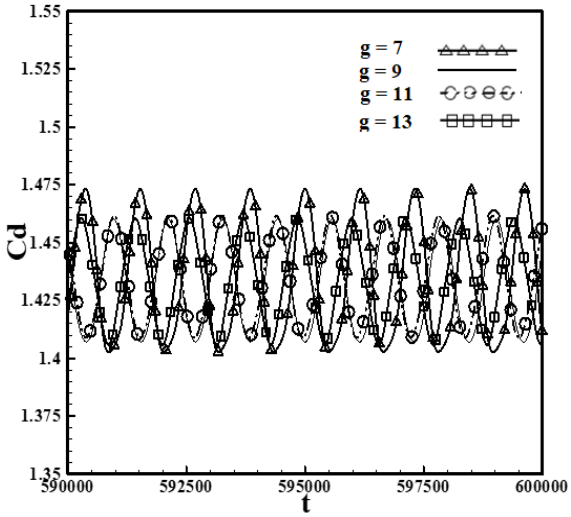


**Fig. 13.** Time-trace of the drag coefficient in the case of a fully developed flow regime.

### *5.3 Effect of partitions length*

#### *5.3.1 Regime flow*

In the literature, a limited number of studies have been performed to investigate the length of the control partition compared to the studies realized to investigate the effect of the gap spacing between the principal cylinder and the control partition. Ali *et al.* (Mat Ali *et al.*, 2011) performed a numerical study on flows around a square cylinder of lateral length $D$ with and without a separator plate at a Reynolds number of 150. In this study, the length of the separator plate varies from $L = 0.5D$ to $L = 6D$. The authors find that the splitter plate introduces a strong hydrodynamic interaction in the wake near the cylinder and that the length of the plate significantly affects the flow structure. Indeed, they observed three flow regimes by varying the length of the separator plate: For short lengths ($0 \lesssim L \lesssim D$), the free shear layers are convex further downstream before curling up as the plate length increases. For intermediate lengths ($1.25D \lesssim L \lesssim 4.75D$), a secondary vortex is clearly visible around the trailing edge of the separating plate, and the shear layers begin to curl

closer to the trailing edge. For longer plate lengths ($L \gtrsim 5D$), a regime in which the free shear layers attach to the separator plate is observed. Another numerical study was performed by Admi *et al.* (Admi *et al.*, 2022b) on fluid flow and thermal convection phenomena around a heated square cylinder controlled by three downstream partitions using the Boltzmann multiple relaxation time network method at a fixed Reynolds number (Re = 150). They find that maximum vortex suppression is observed at a critical length of the control partitions Lp = 4d. The effects of the position and length of a detached downstream plate on the wake of a square cylinder were studied numerically by Ali *et al.* (Ali *et al.*, 2012) at a Reynolds number of 150. The authors identified two flow regimes: the first regime is characterized by the completion of vortex formation downstream of the gap and the second regime is characterized by the completion of vortex formation within the gap. They found that there are abrupt changes in the integral properties observed between regime I and II, with the transition occurring at the critical gap distance Gc = 2.3D. Also, they observed that the plate has no significant effect on the generation of the von Kármán vortex when the separation is beyond ~5.6D.

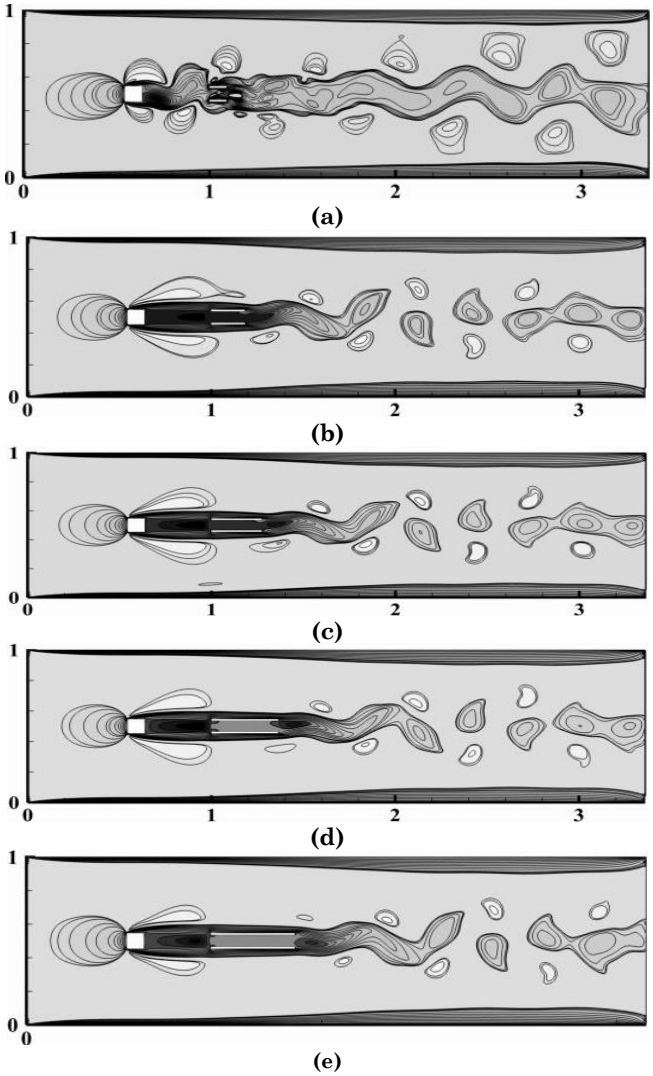


**Fig. 14**. Visualization of instantaneous flow velocity contours for different lenght $1 \leq Lp \leq 5$. (a) Lp = 1d; (b) Lp = 2d; (c) Lp = 3d; (d) Lp = 4d; (e) Lp = 5d.

Figure 14 illustrates the instantaneous velocity contours for six different lengths. These plots make it possible to interpret the topology of the flow reigning around the cylinder controlled by two detached partitions. We observe that there is a very strong generation of vortices behind the plates, particularly in the first case where the flow is disturbed in the gap between the block and the control partitions. This strong generation decreases with increasing partition length, where the size of the vortexes decreases and the regime becomes symmetrical and quasi-stable.

### *5.3.2 Forces statics*

In this section, the effect of the length of the control baffles on the aerodynamic forces is investigated. In this sense, several researches have been carried out. Moussaoui *et al.* (Moussaoui *et al.*, 2010) used LBM to numerically study the incompressible flow around a square cylinder placed downstream of a control bi-partition in a horizontal channel at a Reynolds number of 250. The authors find that the fluid flow exhibits a complex structure in the space between the cylinder and the bi-partition and that the fluid forces acting on the cylinder decrease slightly for the spacing range w/d = 1-4 except for a height h = 0.4 and 0.6. When the position of the control bi-partition w/d =5, the vortex shedding behind the cylinder is almost completely suppressed for small and large values of h, i.e. for h = 0.1-0.3 and 0.8-1.0. Similarly, the authors find that the time-averaged drag tends to decrease gradually as the spacing of the control bi-partitions increases in the range of w/d, except for h = 0.4-0.6. Moreover, for h = 0.8-1.0, the time-averaged drag is negative and it is significantly reduced. It should be noted that the amplitude of fluctuating lift on the square cylinder is successfully suppressed using the control bi-partition, and it can be completely suppressed by carefully choosing the height and position of the control bi-partition. Sakamoto *et al.* (Sakamoto *et al.*, 1997) evaluated the fluid forces acting on a square prism by changing the width of a flat plate and its position on the centre line. They found that the optimum width of the plate for suppression of fluid forces is approximately 10% of that of the prism inserted upstream. Admi *et al.* (Youssef Admi *et al.*, 2022a) find that the maximum percentage reduction in drag coefficient reaches 17.33% when the length of the control plates reaches its critical value (Lp = 4d).

**Table 1**
$Cd_{mean}$ values for different spacing gaps for Lp=3d

| g | $Cd_{mean}$ |
|---|---|
| 0.25 | 1.239 |
| 1 | 1.269 |
| 2 | 1.267 |
| 3.9 | 1.2528 |
| 4 | 1.2520 |
| 9 | 1.441 |

**Table 2**
$Cd_{mean}$ values for different length for g = 4

| Lp | $Cd_{mean}$ |
|---|---|
| 1d | 1.442 |
| 2d | 1.254 |
| 3d | 1.252 |
| 4d | 1.250 |
| 5d | 1.250 |

In this work, to study the effect of the length of the control walls only, we carried out a study on the gap spacing, to find out the optimal position of the two control plates. Also, the Reynolds number was fixed at 150. Six cases are treated when g varies from 0.25 to 9 to get the optimal case of control wall placement. For each g-spacing, we varied the length of the partitions from Lp = 1d to Lp = 5d and considered the case of Lp = 3d as a Cdmean reference. Table 1 shows the average values of the drag coefficient for Lp = 3d. The smallest Cdmean value is found for g = 0.25. However, the average drag coefficient admits high values in the cases where g = 0.25; 1; 2; 9 for all partition lengths except in the case where Lp = 3d. Likewise, Table 2 shows that in the case where g = 4, the average Cd value remains almost constant and takes values of about 1.25 for all lengths (except in the case where Lp = 1d). This is observed in Figure 15, which shows the temporal variation of the drag coefficients.

A difference of less than 0.03% is observed between the $Cd_{mean}$ value for Lp = 2d and for Lp = 5d, where the Cd presents its minimum. This gives the possibility of using partitions of 2d or 3d length instead of using partitions of Lp = 5d length. Since the values of $Cd_{mean}$ are very close, then the lift coefficient values can contribute to the choice of the length of the partitions. From the curve showing the variation of the lift coefficient (Figure 16), it can be seen that it has its maximum for the length Lp = 2d. Therefore, for beneficial flow control, i.e., having reduced values of Cd and high values of Cl, it is preferable to use partitions of length Lp = 2d placed parallel downstream of the cylinder at a position g = 4.

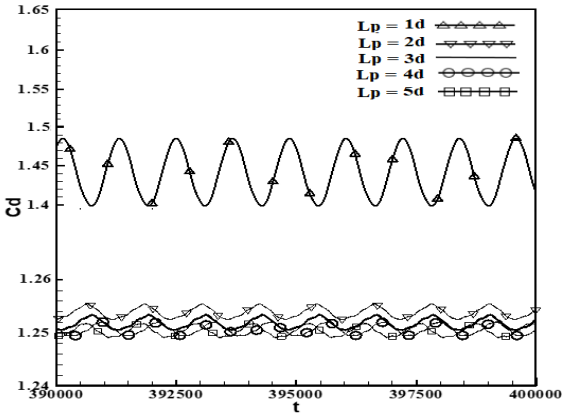


**Fig. 15.** Time-trace of drag coefficient of flow past a square cylinder with detached partitions for different lengths for g=4

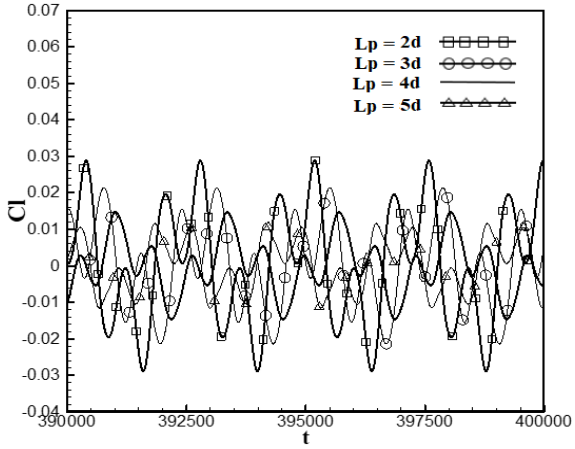


**Fig. 16.** Time-trace of lift coefficient of flow past a square cylinder with detached partitions for different lengths for g = 4.

### *5.4 Effect of partitions position*

#### *5.4.1 Regime flow*

In the last part, we studied the effect of the vertical position of the partitions (i.e. the distance between the two control partitions) for g =1d and Re=150. Figure 17 shows the velocity contour structures for different vertical positions of the partitions. The flow structures show that the presence of the two control partitions introduces a strong hydrodynamic interaction in the wake near the cylinder. This leads to a strong generation of vortices in the wake in all cases tested. In fact, the layers of airborne particles at the edges of the cylinder fall onto the two control plates, and this strong fluid-structure interaction increases the dynamics of the fluid particles in the wake near the cylinder.

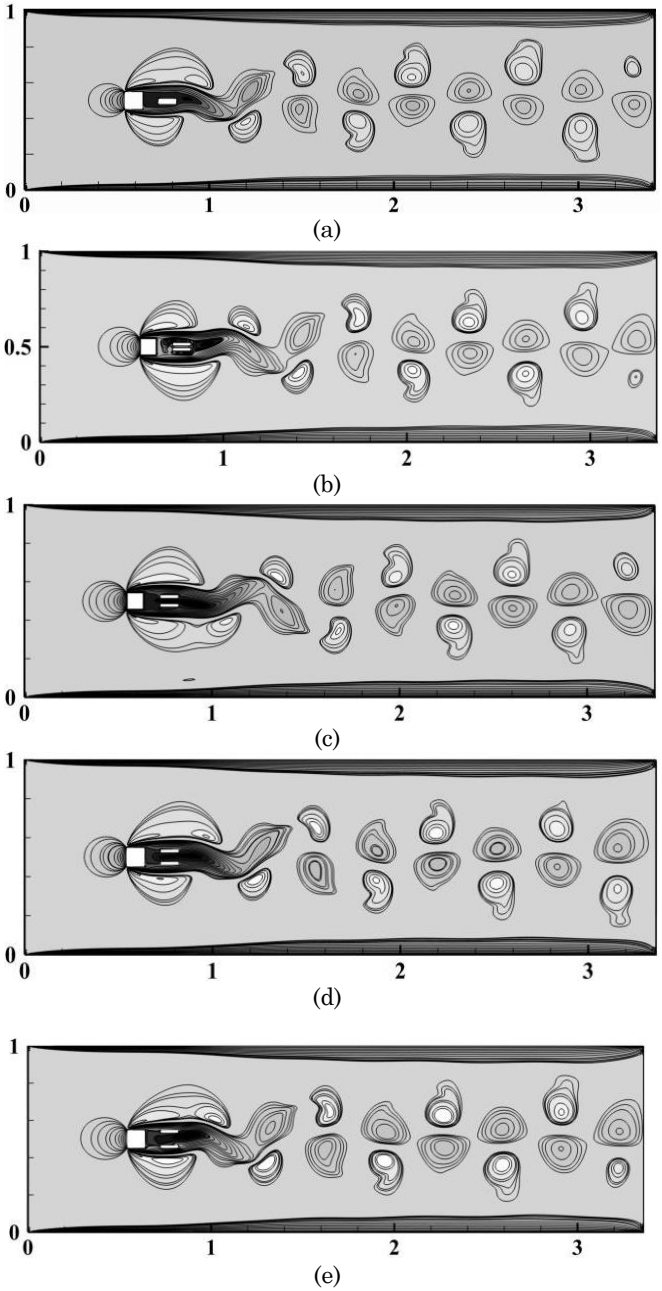


**Fig. 17.** Visualisation of instantaneous flow velocity contours for different vertical gap: (a) a = 0d; (b) a = 0.2d; (c) a = 0.4d; (d) a = 0.6d; (e) a = 0.8d.

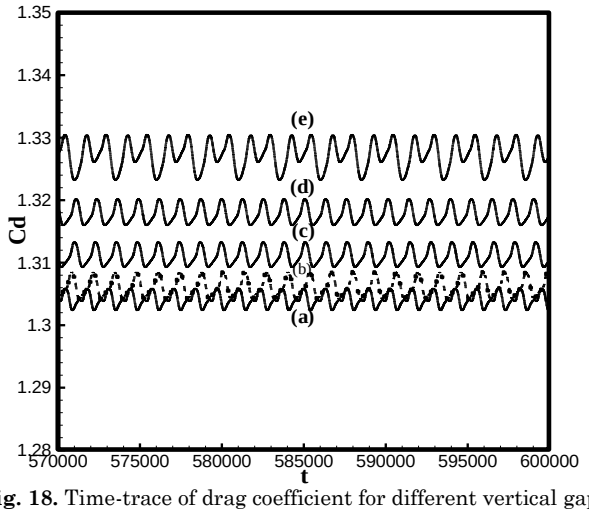


**Fig. 18.** Time-trace of drag coefficient for different vertical gap: (a) a=0.8d; (b) a=0.6d; (c) a=0.4d; (d) a=0.2d; (e) a=0d

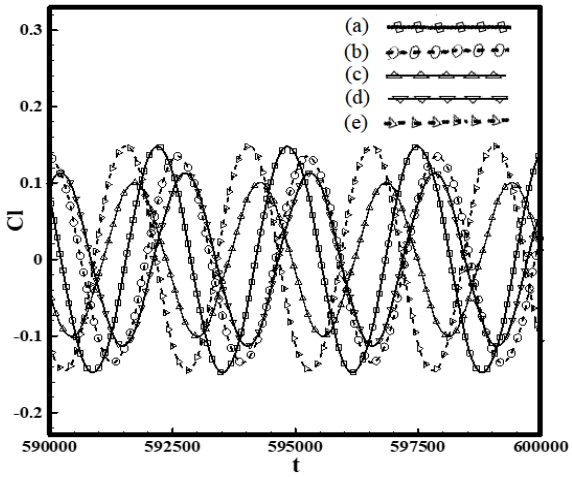


**Fig. 19**. Time-trace of lift coefficient for different vertical gap :(a) a=0.8d; (b) a=0.6d; (c) a=0.4d; (d) a=0.2d; (e) a=0d

### *5.4.2 Forces statics*

Figure 18 presents the variation of the drag coefficient as a function of time for each position of the partitions. From this figure, we see that there is an inversely proportional relationship between the coefficient Cd and the vertical position of the partitions, i.e. the more the distance between the two partitions decreases, the more the value of Cd increases. In the case where the two partitions are associated, the drag coefficient has reached a higher value. This is because the fluid flow delivered by the shear layers strongly interacts with the partitions and causes undulations in the intermediate zone. This increases the fluidic forces acting on the square cylinder. Likewise, the lift coefficient exhibits its greatest value in the case where the detached partitions are placed behind the upper and lower edges of the square cylinder (see Figure 19).

## 5. Conclusions

In this paper, a numerical simulation of the laminar flow of a fluid around a square block arranged in a two-dimensional horizontal channel controlled by two partitions was presented. The numerical approach used is the Lattice Boltzmann method with multiple relaxation times. The study of the effect of the Reynolds number shows that as the Reynolds number increases, the fluidic forces acting on the cylinder decrease until they reach a minimum value at Re = 250 and then start to increase again. Likewise, the root mean square coefficient increases with the Reynolds number. This increase becomes faster for $200 \leq Re \leq 300$. The study of the gap spacing variation at a fixed Reynolds number (Re = 150) shows three different regimes: the extended body regime ($0.25 \leq g \leq 3.9$), the attachment flow regime ($4 \leq g \leq 5.5$), and the fully developed flow regime ($7 \leq g \leq 13$). This study shows that the drag coefficient reaches its minimum Cd = 1.25 at a critical spacing g = 3.9. This shows a reduction of 12.5% compared to the case without a control device. At this critical spacing, a suppression of vortices behind the square cylinder is only observed for the extended body regime. Also, a 12.95% reduction in drag coefficient is achieved for a critical length Lp = 3d. The last study shows that the variation of the distance between the two control partitions shows that the optimal position of the partitions is behind the upper and lower ends of the square cylinder (a = 0.8d). These results show that the control mechanism with simple devices has a significant advantage over the uncontrolled case. For beneficial application in further research in different fields of engineering science, it is recommended to place the two partitions of length Lp= 3d behind the ends of the bluff body at a distance g = 4. This results in a significant energy saving. Note that the extension to 3D calculations and higher Reynolds numbers is being further investigated in ongoing research.

## References

Aabid, A., Afifi, A., Mehaboob Ali, F. A. G., Akhtar, M. N., & Khan, S. A. (2019). CFD analysis of splitter plate on bluff body. *CFD Letters*, 11(11), 25-38.

Admi, Y., Lahmer, E. B., Moussaoui, M. A., & Mezrhab, A. (2022). Effect of a Flat Plate on Drag Force Reduction and Heat Transfer Characteristics Around Three Heated Square Obstacles. *In Journal of Physics: Conference Series* (Vol. 2178, No. 1, p. 012027). IOP Publishing. doi: 10.1088/1742-6596/2178/1/012027

Admi, Y., Moussaoui, M. A., & Mezrhab, A. (2020). Effect of a flat plate on heat transfer and flow past a three side-by-side square cylinders using double MRT-lattice Boltzmann method. *In 2020 IEEE 2nd International Conference on Electronics, Control, Optimization and Computer Science (ICECOCS)* (pp. 1-5). IEEE. doi: 10.1109/ICECOCS50124.2020.9314506

Admi, Y., Moussaoui, M. A., & Mezrhab, A. (2022). Control of Fluid Flow Coupled on Heat Transfer Around a Square Cylinder by Using Three Attached Partitions. *In International Conference on Digital Technologies and Applications* (pp. 845-854). Springer, Cham. Doi: 10.1007/978-3-031-01942-5_84

Admi, Y., Moussaoui, M. A., & Mezrhab, A. (2021). Effect of Control Partitions on Drag Reduction and Suppression of Vortex Shedding Around a Bluff Body Cylinder. *In International Conference on Advanced Technologies for Humanity* (pp. 453-463). Springer, Cham. doi: 10.1007/978-3-030-94188-8_40

Admi, Y., Moussaoui, M. A., & Mezrhab, A. (2022). The Vortex Shedding Suppression and Heat Transfer Characteristics Around a Heated Square Cylinder by Using Three Downstream-Detached Partitions. *In International Conference on Digital Technologies and Applications* (pp.

598-608). Springer, Cham. Doi : 10.1007/978-3-031-02447-4_62

Admi, Y., Moussaoui, A. M. (2022). Numerical Investigation of Convective Heat Transfer and Fluid Flow Past a Three-SquareCylinders Controlled by a Partition in Channel. *Int. J. Renew. Energy Dev*, 11(3), 766–781.

Ali, M. S. M., Doolan, C. J., & Wheatley, V. (2012). Low Reynolds number flow over a square cylinder with a detached flat plate. *International Journal of Heat and Fluid Flow*, 36, 133-141. doi: 10.1016/j.ijheatfluidflow.2012.03.011

Alonzo-Garcia, A., Cuevas-Martinez, J., Gutiérrez-Torres, C. D. C., Jiménez-Bernal, J. A., Martinez-Delgadillo, S. A., & Medina-Pérez, R. (2021). The control of unsteady forces and wake generated in circular and square cylinder at laminar periodic regime by using different rod geometries. *Ocean Engineering*, 233, 109121. doi: 10.1016/j.oceaneng.2021.109121

Anderson, E. A., & Szewczyk, A. A. (1997). Effects of a splitter plate on the near wake of a circular cylinder in 2 and 3-dimensional flow configurations. *Experiments in Fluids*, 23(2), 161-174. doi: 10.1007/s003480050098

Apelt, C. J., & West, G. S. (1975). The effects of wake splitter plates on bluff-body flow in the range 104< R< 5× 104. Part 2. *Journal of Fluid Mechanics*, 71(1), 145-160. doi: 10.1017/S0022112075002479

Apelt, C. J., West, G. S., & Szewczyk, A. A. (1973). The effects of wake splitter plates on the flow past a circular cylinder in the range $10^4$<R<$5\times10^4$. *Journal of Fluid Mechanics*, 61(1), 187–198. doi: 10.1017/S0022112073000649

Mooneghi, M. A., & Kargarmoakhar, R. (2016). Aerodynamic mitigation and shape optimization of buildings. *Journal of building engineering*, 6, 225-235. doi: 10.1016/j.jobe.2016.01.009

Bao, Y., & Tao, J. (2013). The passive control of wake flow behind a circular cylinder by parallel dual plates. *Journal of Fluids and Structures*, 37, 201-219. doi: 10.1016/j.jfluidstructs.2012.11.002

Benhamou, J., Admi, Y., Jami, M., Moussaoui, M. A., & Mezrhab A. (2022). 3D Simulation of Natural Convection in a Cubic Cavity with Several Differentially Heated Walls. *In 2022 2nd International Conference on Innovative Research in Applied Science, Engineering and Technology (IRASET)* (pp. 1-7). IEEE doi: 10.1109/iraset52964.2022.9738080

Benhamou, J., & Jami, M. (2022). Three-dimensional numerical study of heat transfer enhancement by sound waves using mesoscopic and macroscopic approaches. *Heat Transfer* 51(5), 3892-3919. doi: 10.1002/htj.22482

Benhamou, J., Jami, M., Mezrhab, A., Botton, V., & Henry, D. (2020). Numerical study of natural convection and acoustic waves using the lattice Boltzmann method. *Heat Transfer*, 49(6), 3779-3796. doi: 10.1002/htj.21800

Bhatnagar, P. L., Gross, E. P., & Krook, M. (1954). A model for collision processes in gases. I. Small amplitude processes in charged and neutral one-component systems. *Physical review*, 94(3), 511. doi: 10.1103/PhysRev.94.511

Bouzidi, M. H., Firdaouss, M., & Lallemand, P. (2001). Momentum transfer of a Boltzmann-lattice fluid with boundaries. *Physics of fluids*, 13(11), 3452-3459. doi: 10.1063/1.1399290

Breuer, M., Bernsdorf, J., Zeiser, T., & Durst, F. (2000). Accurate computations of the laminar flow past a square cylinder based on two different methods: lattice-Boltzmann and finite-volume. *International journal of heat and fluid flow*, 21(2), 186-196. doi: 10.1016/S0142-727X(99)00081-8

Bruneau, C. H., Creusé, E., Gilliéron, P., & Mortazavi, I. (2014). A glimpse on passive control using porous media for incompressible aerodynamics. *Int. J. Aerodyn*, 4(1/2), 70. doi: 10.1504/ijad.2014.057806

Chauhan, M. K., Dutta, S., & Gandhi, B. K. (2019). Wake flow modification behind a square cylinder using control rods. *Journal of Wind Engineering and Industrial Aerodynamics*, 184, 342-361. doi: 10.1016/j.jweia.2018.12.002

Chiarini, A., & Quadrio, M. (2021). The turbulent flow over the BARC rectangular cylinder: A DNS study. *Flow, Turbulence and Combustion*, 107(4), 875-899. doi: 10.1007/s10494-021-00254-1

d'Humières, D. (2002). Multiple–relaxation–time lattice Boltzmann models in three dimensions. Philosophical Transactions of the Royal Society of London. Series A: *Mathematical, Physical and Engineering Sciences*, 360(1792), 437-451. doi: 10.1098/rsta.2001.0955

Dehkordi, B. G., & Jafari, H. H. (2011). Numerical analysis on the effect of embedding detached short splitter-plates in the downstream of a circular cylinder. *Progress in Computational Fluid Dynamics, an International Journal*, 11(1), 6-17. doi: 10.1504/PCFD.2011.037568

Ding, L., Mao, X., Yang, L., Yan, B., Wang, J., & Zhang, L. (2021). Effects of installation position of fin-shaped rods on wind-induced vibration and energy harvesting of aeroelastic energy converter. *Smart Materials and Structures*, 30(2), 025026. doi: 10.1088/1361-665X/abd42b

Doolan, C. J. (2009). Flat-plate interaction with the near wake of a square cylinder. *AIAA journal*, 47(2), 475-479. doi: 10.2514/1.40503

Fatahian, E., Nichkoohi, A. L., & Fatahian, H. (2019). Numerical study of the effect of suction at a compressible and high Reynolds number flow to control the flow separation over Naca 2415 airfoil. *Progress in Computational Fluid Dynamics, an International Journal*, 19(3), 170-179. doi: 10.1504/pcfd.2019.099598

Feng, Z. G., & Michaelides, E. E. (2001). Drag coefficients of viscous spheres at intermediate and high Reynolds numbers. J. *Fluids Eng.*, 123(4), 841-849. doi: 10.1115/1.1412458

Frisch, U., Hasslacher, B., & Pomeau, Y. (2019). Lattice-gas automata for the Navier-Stokes equation. In Lattice Gas Methods for Partial Differential Equations (pp. 11-18). *CRC Press*. doi: 10.1103/PhysRevLett.56.1505

Gilliéron, P. (2002). Flow control applied to the car. State of the art. *Mcanique & Industries*, 3(6), 515–524. doi: 10.1016/S1296-2139(02)01197-1

Gupta, A., & Saha, A. K. (2019). Suppression of vortex shedding in flow around a square cylinder using control cylinder. *European Journal of Mechanics, B/Fluids*, 76, 276–291. doi: 10.1016/j.euromechflu.2019.03.006

Saraei, S. H., Chamkha, A., & Dadvand, A. (2021). Controlling the hydrodynamic forces on a square cylinder in a channel via an upstream porous plate. *Mathematics and Computers in Simulation*, 185, 272-288. doi: 10.1016/j.matcom.2020.12.017

Islam, S. Ul, Rahman, H., Abbasi, W. S., & Shahina, T. (2015). Lattice Boltzmann Study of Wake Structure and Force Statistics for Various Gap Spacings Between a Square Cylinder with a Detached Flat Plate. *Arabian Journal for Science and Engineering*, 40(8), 2169–2182. doi: 10.1007/s13369-015-1648-3

Islam, S. U., Manzoor, R., Islam, Z. U., Kalsoom, S., & Ying, Z. C. (2017). A computational study of drag reduction and vortex shedding suppression of flow past a square cylinder in presence of small control cylinders. *AIP Advances*, 7(4), 045119. doi: 10.1063/1.4982696

Islam, S. U., Rahman, H., Abbasi, W. S., Noreen, U., & Khan, A. (2014). Suppression of fluid force on flow past a square cylinder with a detached flat plate at low Reynolds number for various spacing ratios. *Journal of Mechanical science and Technology*, 28(12), 4969-4978. doi: 10.1007/s12206-014-1118-y

Lahmer, E. B., Admi, Y., Moussaoui, M. A., & Mezrhab, A. (2022). Improvement of the heat transfer quality by air cooling of three-heated obstacles in a horizontal channel using the lattice Boltzmann method. *Heat Transfer*, 51(5), 3869-3891. doi: 10.1002/htj.22481

Lahmer, E. B., Benhamou, J., Admi, Y., moussaoui, mohammed amine, Jami, M., Mezrhab, A., & Phanden, R. K. (2022). Convective and Conjugate Heat Transfer Efficiency Enhancement over Partitioned Channel within Backward-Facing Step using the Lattice Boltzmann Method LBM-

DMRT. *Journal of Enhanced Heat Transfer*, 29(3), 51–77. doi: 10.1615/jenhheattransf.2022040357

Lallemand, P., & Luo, L. S. (2000). Theory of the lattice Boltzmann method: Dispersion, dissipation, isotropy, Galilean invariance, and stability. *Physical review E*, 61(6), 6546. doi: 10.1103/PhysRevE.61.6546

Li, D., Wu, Y., Da Ronch, A., & Xiang, J. (2016). Energy harvesting by means of flow-induced vibrations on aerospace vehicles. *Progress in Aerospace Sciences*, 86, 28-62. doi: 10.1016/j.paerosci.2016.08.001

Liu, K., Deng, J., & Mei, M. (2016). Experimental study on the confined flow over a circular cylinder with a splitter plate. *Flow Measurement and Instrumentation*, 51, 95-104. doi: 10.1016/j.flowmeasinst.2016.09.002

Loh, S. K., Faris, W. F., & Hamdi, M. (2013). Fluid-structure interaction simulation of transient turbulent flow in a curved tube with fixed supports using LES. *Progress in Computational Fluid Dynamics, an International Journal*, 13(1), 11-19. doi: 10.1504/PCFD.2013.050646

Maruai, N. M., Mat Ali, M. S., Ismail, M. H., & Shaikh Salim, S. A. Z. (2018). Downstream flat plate as the flow-induced vibration enhancer for energy harvesting. *Journal of Vibration and Control*, 24(16), 3555-3568. doi: 10.1177/1077546317707877

Mat Ali, M. S., Doolan, C. J., & Wheatley, V. (2011). Low Reynolds number flow over a square cylinder with a splitter plate. *Physics of Fluids*, 23(3), 033602. doi: 10.1063/1.3563619

Mezrhab, A., Moussaoui, M. A., Jami, M., Naji, H., & Bouzidi, M. H. (2010). Double MRT thermal lattice Boltzmann method for simulating convective flows. *Physics Letters A*, 374(34), 3499-3507. doi: 10.1016/j.physleta.2010.06.059

Mohamad, A. A. (2011). Fundamentals and engineering applications with computer codes. *Springer*.

Moussaoui, M. A., Admi, Y., Lahmer, E. B., & Mezrhab, A. (2021, February). Numerical investigation of convective heat transfer in fluid flow past a tandem of triangular and square cylinders in channel. *In IOP Conference Series: Materials Science and Engineering* (Vol. 1091, No. 1, p. 012058). IOP Publishing. doi: 10.1088/1757-899x/1091/1/012058

Moussaoui, M. A., Jami, M., Mezrhab, A., Naji, H., & Bouzidi, M. (2010). Multiple-relaxation-time lattice Boltzmann computation of channel flow past a square cylinder with an upstream control bi-partition. *International journal for numerical methods in fluids*, 64(6), 591-608. doi: 10.1002/fld.2159

Moussaoui, M. A., Jami, M., Mezrhab, A., Naji, H., & Bouzidi, M. (2010). Multiple-relaxation-time lattice Boltzmann computation of channel flow past a square cylinder with an upstream control bi-partition. *International journal for numerical methods in fluids*, 64(6), 591-608. doi: 10.1109/WITS.2019.8723863

Moussaoui, M. A., Mezrhab, A., & Naji, H. (2011). A computation of flow and heat transfer past three heated cylinders in a vee shape by a double distribution MRT thermal lattice Boltzmann model. *International journal of thermal sciences*, 50(8), 1532-1542. doi: 10.1016/j.ijthermalsci.2011.03.011

Nidhul, K., Sunil, A. S., & Kishore, V. (2015). Numerical Investigation of Flow Characteristics over a Square Cylinder with a Detached Flat Plate of Varying Thickness at Critical Gap Distance in the wake at Low Reynolds Number. *International Journal of Research in Aeronautical and Mechanical Engineering*, 3(1), 104–118.

Okajima, A. (1982). Strouhal numbers of rectangular cylinders. *Journal of Fluid mechanics*, 123, 379-398.

Ozono, S. (1999). Flow control of vortex shedding by a short splitter plate asymmetrically arranged downstream of a cylinder. *Physics of Fluids*, 11(10), 2928-2934. doi: 10.1063/1.870151

Park, Y. G., Yoon, H. S., & Ha, M. Y. (2013). Numerical study on the laminar fluid flow characteristics around a rectangular cylinder with different width to height ratios. *Progress in Computational Fluid Dynamics, an International Journal*, 13(3-4), 244-262. doi: 10.1504/PCFD.2013.053670

Qian, Y. H., d'Humières, D., & Lallemand, P. (1992). Lattice BGK models for Navier-Stokes equation. EPL (*Europhysics Letters*), 17(6), 479. doi: 10.1209/0295-5075/17/6/001

Rashidi, S., Hayatdavoodi, M., & Esfahani, J. A. (2016). Vortex shedding suppression and wake control: A review. *Ocean Engineering*, 126, 57-80. doi: 10.1016/j.oceaneng.2016.08.031

Roshko, A. (1954). On the drag and shedding frequency of two-dimensional bluff bodies (No. NACA-TN-3169).

Saha, A. K., Biswas, G., & Muralidhar, K. (2003). Three-dimensional study of flow past a square cylinder at low Reynolds numbers. *International Journal of Heat and Fluid Flow*, 24(1), 54-66. doi: 10.1016/S0142-727X(02)00208-4

Sakamoto, H., Tan, K., Takeuchi, N., & Haniu, H. (1997). Suppression of fluid forces acting on a square prism by passive control. *Journal of Fluids Engineering, Transactions of the ASME*, 119(3): 506-511. doi: 10.1115/1.2819273

Sohankar, A., Norberg, C., & Davidson, L. (1999). Simulation of three-dimensional flow around a square cylinder at moderate Reynolds numbers. *Physics of fluids*, 11(2), 288-306.

Turki, S. (2008). Numerical simulation of passive control on vortex shedding behind square cylinder using splitter plate. *Engineering Applications of Computational Fluid Mechanics*, 2(4), 514-524. doi: 10.1080/19942060.2008.11015248

Vamsee, G. R., De Tena, M. L., & Tiwari, S. (2014). Effect of arrangement of inline splitter plate on flow past square cylinder. *Progress in Computational Fluid Dynamics, an International Journal*, 14(5), 277-294. doi: 10.1504/PCFD.2014.064554

You, D., Choi, H., Choi, M. R., & Kang, S. H. (1998). Control of flow-induced noise behind a circular cylinder using splitter plates. *AIAA journal*, 36(11), 1961-1967. doi: 10.2514/2.322

Yu, Z., Ping, H., Liu, X., Zhu, H., Wang, R., Bao, Y., ... & Xu, H. (2020). Turbulent wake suppression of circular cylinder flow by two small counter-rotating rods. *Physics of Fluids*, 32(11), 115123. doi: 10.1063/5.0023881

Zhong, W., Yim, S. C., & Deng, L. (2020). Vortex shedding patterns past a rectangular cylinder near a free surface. *Ocean Engineering*, 200, 107049. doi: 10.1016/j.oceaneng.2020.107049

Zhou, L., Cheng, M., & Hung, K. C. (2005). Suppression of fluid force on a square cylinder by flow control. *Journal of Fluids and Structures*, 21(2), 151-167. doi: 10.1016/j.jfluidstructs.2005.07.002

Zhu, H., & Liu, W. (2020). Flow control and vibration response of a circular cylinder attached with a wavy plate. *Ocean Engineering*, 212, 107537. doi: 10.1016/j.oceaneng.2020.107537

Zou, Q., & He, X. (1997). On pressure and velocity boundary conditions for the lattice Boltzmann BGK model. *Physics of fluids*, 9(6), 1591-1598. doi: 10.1063/1.869307